

## Transport out of the lower stratospheric Arctic vortex by Rossby wave breaking

D. W. Waugh,<sup>1</sup> R. A. Plumb,<sup>1</sup> R. J. Atkinson,<sup>1</sup> M. R. Schoeberl,<sup>2</sup> L. R. Lait,<sup>2</sup>  
P. A. Newman,<sup>2</sup> M. Loewenstein,<sup>3</sup> D. W. Toohey,<sup>4</sup> L. M. Avallone,<sup>5</sup>  
C. R. Webster,<sup>6</sup> and R. D. May<sup>6</sup>

**Abstract.** The fine-scale structure in lower stratospheric tracer transport during the period of the two Arctic Airborne Stratospheric Expeditions (January and February 1989; December 1991 to March 1992) is investigated using contour advection with surgery calculations. These calculations show that Rossby wave breaking is an ongoing occurrence during these periods and that air is ejected from the polar vortex in the form of long filamentary structures. There is good qualitative agreement between these filaments and measurements of chemical tracers taken aboard the NASA ER-2 aircraft. The ejected air generally remains filamentary and is stretched and mixed with midlatitude air as it is wrapped around the vortex. This process transfers vortex air into midlatitudes and also produces a narrow region of fine-scale filaments surrounding the polar vortex. Among other things, this makes it difficult to define a vortex edge. The calculations also show that strong stirring can occur inside as well as outside the vortex.

### 1. Introduction

It has been argued that the observed ozone depletion in northern hemisphere midlatitudes over the past decade [e.g., Stolarski *et al.*, 1991, 1992] may be due to the transport of chemically perturbed air from within the polar vortex to midlatitudes [e.g., Tuck *et al.*, 1992]. Through Rossby wave breaking [McIntyre and Palmer, 1983, 1984, 1985], air is ejected from the vortex and mixed into the surrounding surf zone. The air is usually stripped from the vortex edge, eroding the vortex and steepening the isentropic gradients of potential vorticity (PV) that mark the edge [Dritschel, 1988; Legras and Dritschel, 1993]. This wave breaking, mixing, and edge sharpening are observed in high-resolution numerical simulations [e.g., Juckes and McIntyre, 1987; Salby *et al.*, 1990; Polvani and Plumb, 1992; Waugh, 1992; Norton, 1993; Pierce and Fairlie, 1993], but the scales involved in these processes are generally smaller than those of current meteorological analyses. Therefore it has not been possible to investigate in detail wave breaking in the stratosphere, and there are many unanswered questions. For example, how often does wave breaking occur in the stratosphere, how much air is ejected from the vortex during wave breaking, and how rapidly is this vortex air mixed with midlatitude air?

Some insight into the fine-scale structure in the lower

stratospheric tracer transport has been gained through aircraft measurements of chemical tracers made during the Airborne Antarctic Ozone Experiment and the Airborne Arctic Stratospheric Expeditions (AASE 1 and 2); see the special issues of *Journal of Geophysical Research* (vol. 94 (D9, D14) 1989), *Geophysical Review Letters* (vol. 17, 1990), and *Science* (vol. 261, 1993). These measurements have shown evidence of a sharp vortex edge and also, from several flights, evidence of the existence of small-scale features outside the polar vortex having the same chemical signature as air from inside the vortex.

Tuck *et al.* [1992] investigated transport out of the lower stratospheric polar vortex during the period of the AASE 1 using aircraft measurements together with European Centre for Medium-Range Weather Forecast (ECMWF) analyses and a limited number of back trajectory calculations. The ECMWF analyses typically show small-scale "blobs" of high PV outside the vortex. Tuck *et al.* [1992] concluded that these blobs had originated from inside the vortex and that a significant amount of air is exported. However, there are doubts about the reality of these small-scale features in the operational analyses [Carver *et al.*, 1993; A. J. Simmons, private communication, 1993]. Moreover, the blobs do not resemble the most typical structures produced by wave breaking in high-resolution numerical simulations.

In this paper we examine tracer transport using the contour advection with surgery (CAS) trajectory technique [Waugh and Plumb, 1993; Norton, 1993]. This technique permits examination of the tracer transport at scales much smaller than those of meteorological analyses and permits a much closer and more systematic examination of the wave breaking and mixing occurring in the stratosphere. It can be viewed as a sophisticated further development of the trajectory technique. A brief description of CAS is given in the next section; for full details, including demonstrations of the accuracy of the technique, see work by D. W. Waugh and R. A. Plumb (submitted manuscript, 1993). We concentrate

<sup>1</sup>Center for Meteorology and Physical Oceanography, Massachusetts Institute of Technology, Cambridge.

<sup>2</sup>NASA Goddard Space Flight Center, Greenbelt, Maryland.

<sup>3</sup>NASA Ames Research Center, Moffett Field, California.

<sup>4</sup>Department of Geosciences, University of California, Irvine.

<sup>5</sup>Department of Chemistry, Harvard University, Cambridge, Massachusetts.

<sup>6</sup>Jet Propulsion Laboratory, Pasadena, California.

on transport occurring during the periods of the two AASE missions (January and February 1989; December 1991 to March 1992). This permits comparison of the results of CAS calculations with the aircraft measurements of chemical tracers.

Details of the procedure used in this paper to analyze the tracer transport are described in the next section. Then in sections 3 and 4 we examine the evolution of the vortex during periods in which air with the signature of vortex air was detected outside the vortex by measurements aboard the NASA ER-2 aircraft. The CAS calculations suggest that wave breaking was almost always occurring during these periods and that air was being ejected from the polar vortex in the form of filamentary strands. This ejected air was stretched and wrapped around the vortex, forming narrow filamentary regions around the vortex. The stability of these filaments is discussed in section 5. The CAS calculations also suggest that strong stirring can occur inside the Arctic vortex. This stirring, together with the amount of air transported out of the vortex, is quantified in section 6. In the final section we briefly discuss the implications for the modeling of stratospheric chemistry. We also discuss the reality or otherwise of the midlatitude blobs of high-PV air appearing in meteorological stratospheric analyses and the differences between vortex evolution in the middle and lower stratosphere.

In this paper we concentrate on the transport of air out of the vortex. During winter 1991–1992 there were also events in which air was entrained into the vortex; these events are examined in a companion paper [Plumb *et al.*, this issue].

## 2. Method of Analysis

Full details and sensitivity tests of the CAS technique are given by Waugh and Plumb [1993], and only a brief description is given here. Comparisons of CAS with the high-resolution ECMWF forecast model and with in situ data from instruments on the NASA DC-8 and ER-2 aircrafts are presented by Plumb *et al.* [this issue].

CAS traces the evolution of specified material contours by representing the contours by a series of material particles and advecting these particles by the wind interpolated from the specified gridded distribution. The resolution of the contours is preserved by automatically adjusting the number of particles (e.g., by placing additional particles in regions of high curvature). At the same time, the number of particles is maintained at a computationally manageable level by including a "surgery" procedure that disconnects and reconnects contours when the scale of features is below some prescribed surgery scale. In the calculations presented, this surgery scale is approximately 8 km (the numerical parameters  $\mu = 0.10$  and  $\delta = 0.00125$  are used in the surgery algorithm [see Dritschel, 1989a]). The contour representation and surgery are the same as in the contour surgery technique developed by Dritschel [1989a].

The CAS calculations in this paper use National Meteorological Center (NMC) stratospheric analyses ( $4^\circ$  latitude  $\times$   $5^\circ$  longitude for 1989;  $2^\circ$  latitude  $\times$   $5^\circ$  longitude for 1991–1992). The initial contours in the calculations are specified to coincide with the 1200 UT analyzed positions of the contours of Ertel PV on the given isentropic surface, and the contours are advected by the daily NMC-analyzed winds on that surface (440 or 500 K for 1989; 450 K for 1991–1992). Only

contours corresponding to the polar vortex are retained in the initial data; all contours in the surrounding surf zone are removed even if the analyzed PV values apparently correspond to air from within the polar vortex. Thus we focus attention on transport out of the vortex during the period considered.

To confirm the reality of the fine-scale structure shown in the CAS calculations, we have compared these structures with measurements made aboard the ER-2. During the AASE missions the ER-2 made flights at approximately constant potential temperature into the vortex and made in situ measurements of numerous chemical tracers and meteorological quantities. We compare the structures of these measurements, in particular those of the mixing ratios of ClO [Toohey *et al.*, 1991, 1993] and N<sub>2</sub>O, from either the ATLAS [Loewenstein *et al.*, 1989, 1990] or the ALIAS [Webster *et al.*, 1993] instrument, with that of the material contours from CAS calculations. High ClO is a signature of chemically perturbed air, while low N<sub>2</sub>O is characteristic of vortex air. We define regions where there is both high ClO and low N<sub>2</sub>O as perturbed vortex air, and we compare observations of this air with the filamentary structures in CAS calculations.

Although CAS calculations covering the entire period of each mission have been performed, we concentrate on periods when ER-2 measurements show perturbed vortex air outside the vortex. The main periods considered are February 7 to 10, 1989; February 20 and 21, 1989; and January 4 to 8, 1992. In the remainder of this paper, all maps shown correspond to 1200 UT on the given date, and PV is in units of  $10^{-6} \text{ K m}^2 \text{ s}^{-1} \text{ kg}^{-1}$ .

## 3. Filamentary Wave Breaking

In this section we consider two periods (January 4–8, 1992, and February 7–10, 1989) during which several ER-2 flights observed perturbed vortex air outside the vortex. CAS calculations during these periods support the idea that this air had been ejected from the vortex during filamentary wave-breaking events.

The results of a 450 K CAS calculation from December 26, 1991, to January 8, 1992, are shown in Figure 1a. This calculation shows that during this period there were two large wave-breaking events in which air was ejected from the vortex in the form of long filamentary structures (e.g., one over Canada and another over Russia on January 4, 1992). The large-scale structure of the vortex in the CAS calculation is consistent with the NMC analyses (see Figure 1b), but there are marked differences at small scales. The analyses, although suggesting the occurrence of wave breaking, do not show the filamentary structure of the breaking (in particular, the filaments around the vortex from January 4 to 8, 1992). Furthermore, the gradients at the edge of the analyzed vortex are not as steep as in the CAS calculation. These differences are, however, consistent with the view that the analyses give only a low-resolution picture of the real stratosphere and do not capture fine-scale structures.

In the CAS calculation the air ejected from the vortex remains filamentary and shows no sign of rolling up into vortices; this lack of "roll-up" and stability of the ejected filamentary structures is discussed further in section 5. The filaments are mainly wrapped around the vortex, although some air does end up in midlatitudes. The CAS calculation has been continued until January 10, 1992, at which stage the

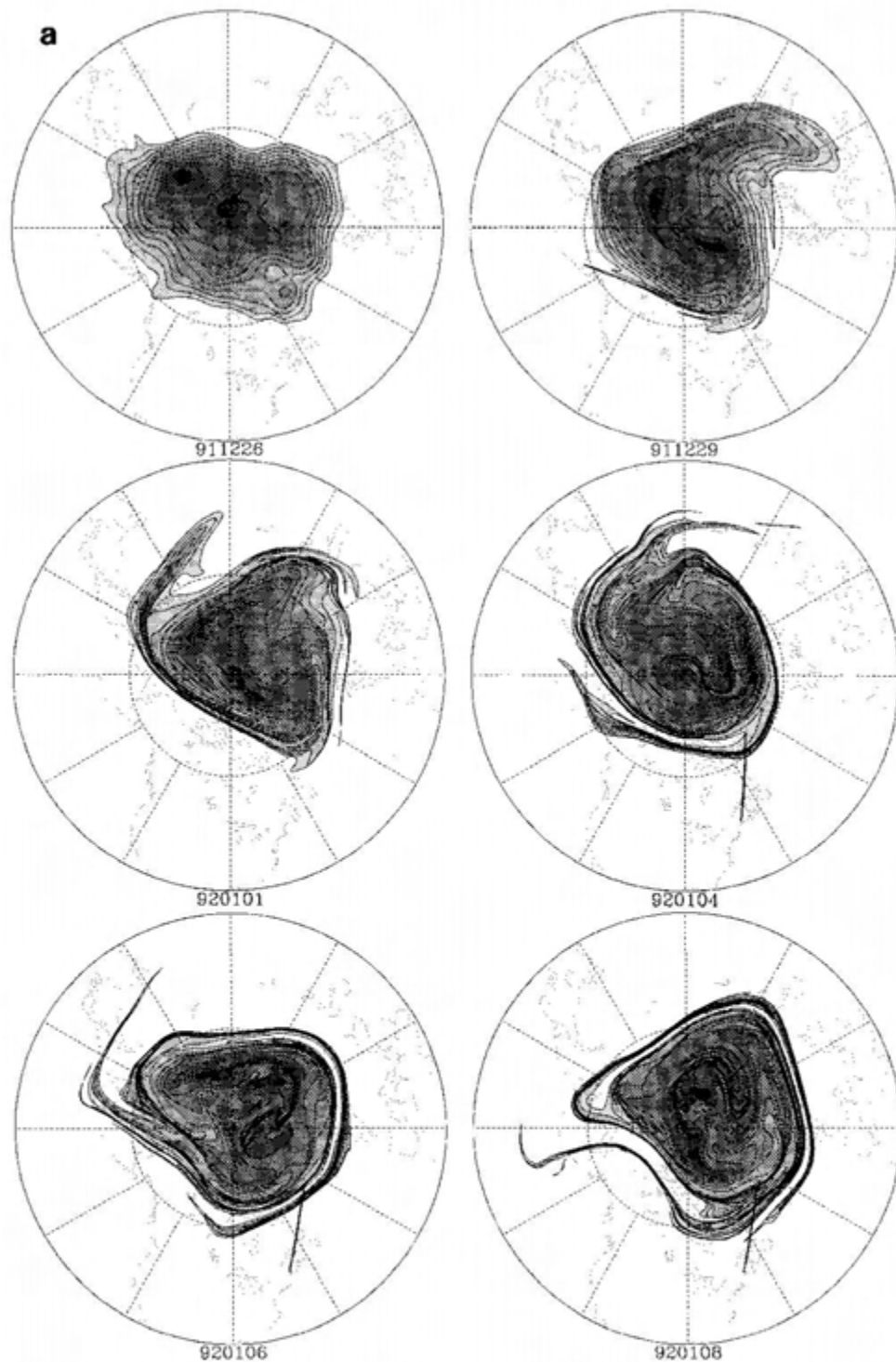


**Figure 1.** (a) Results of a CAS calculation from 1200 UT, December 26, 1991, using NMC-analyzed winds on the 450 K isentropic surface. The initial contours are put at the analyzed locations of the  $(20, 22, 24, \dots) \times 10^{-6} \text{ K m}^2 \text{ s}^{-1} \text{ kg}^{-1}$  contours of Ertel PV on the 450 K surface. The ER-2 flight path is marked for the flights on January 4, 6, and 8. (b) Ertel PV on the 450 K surface from NMC analyses at 1200 UT on December 29, 1991, and January 1, 6, and 8, 1992. Contour levels are the same as in Figure 1a. North polar stereographic projections; 90°W is at bottom of figure.

end of one filament is as far south as 30°N. Furthermore, the filaments thin and lengthen with time, and the interfacial surface area between ex-vortex and midlatitude air increases and hence enhances the diffusional mixing of the two air

masses (see section 6 for further discussion). An important feature of the calculation in Figure 1 is that there is stirring inside as well as outside the vortex. Note that the internal structure in NMC analyses hints that there may be interior

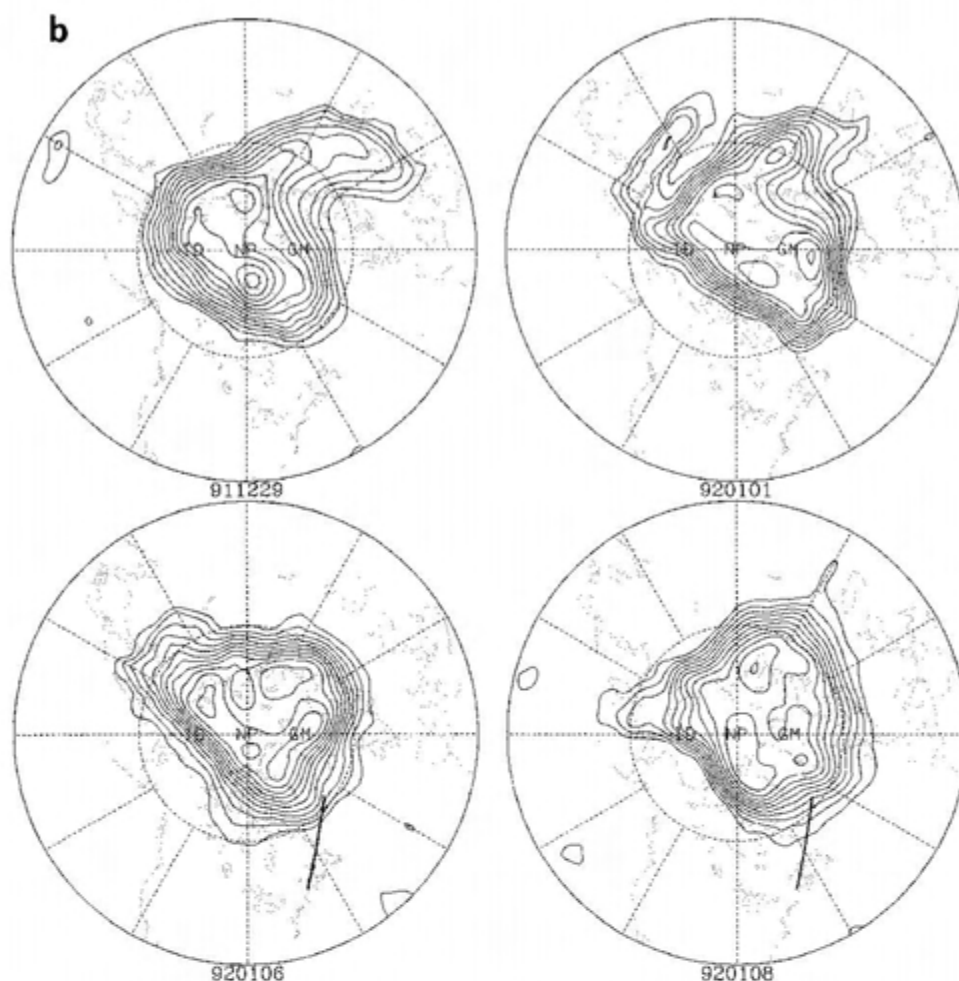


Figure 1. (continued)

stirring. The rate of stirring both inside and outside the vortex is quantified in section 6.

During this period there were three ER-2 flights north from Bangor, Maine ( $45^{\circ}\text{N}$ ,  $69^{\circ}\text{W}$ ), into the vortex, on January 4, 6, and 8, 1992; flight paths are shown in Figure 1. The CAS calculation shown in Figure 1 suggests that on each of these flights the ER-2 crossed filaments of air ejected from the vortex. On the first two flights a single filament was crossed when it was clear of the vortex, whereas on the third flight the path crossed several filaments, including the tip of the filament crossed on the two previous flights.

The observed mixing rates of  $\text{ClO}$  and  $\text{N}_2\text{O}$  for the northbound legs of these three flights are shown in Figure 2; the data from the return leg show a similar structure. The measurements of  $\text{ClO}$  and  $\text{N}_2\text{O}$  on the flights of January 4 and 6, 1992, show a narrow region of perturbed vortex air (e.g., high  $\text{ClO}$  and low  $\text{N}_2\text{O}$ ) at around  $\text{UT} = 57,000$  s. This region is approximately 400 km wide (when converting elapsed time to distance, we use 200 m/s as the nominal speed of the ER-2) and is consistent with the picture given by CAS of a filament of vortex air outside the vortex. The observations also show a region of perturbed vortex air at the turning points of both flights. The CAS calculation suggests that these features region corresponded to the points at which the ER-2 penetrated the outside edge of the vortex (see Figure 1a for January 4 and 6, 1992).

To compare more closely the tracer measurements and the CAS calculations, we have calculated the structures along the three flight paths as determined from the CAS calculation, assuming that we may assign the value of the PV in the initial distribution to each contour. These structures are shown at the bottom of Figure 2. Also shown is the PV from the NMC analyses; note that there are no NMC analyses for January 4, 1992. There is good qualitative agreement between the structure determined from CAS and the observed chemical tracers: there is a narrow region of perturbed vortex air at approximately  $\text{UT} = 57,000$  s and also at the end of the northbound leg for the flight on January 6, 1992. There is no perturbed vortex air at the turning point of the January 4, 1992, flight, but as shown in Figure 1a, the edge of the vortex as predicted by the CAS calculation is just outside the flight path. Although the filament in the CAS calculation is in roughly the same position as in the chemical observations, it is thinner than the observed structure. Note that it is difficult to compare quantitatively the CAS calculation with the chemical tracers, as the initial tracer distribution is not known, and therefore it is not known which contour corresponds to the edge of the region of perturbed air. The sensitivity of the position and width of the filament to the duration of the CAS calculation is discussed below.

The results from the CAS calculation shown in Figure 1 suggest that the structure of the chemical tracers on the

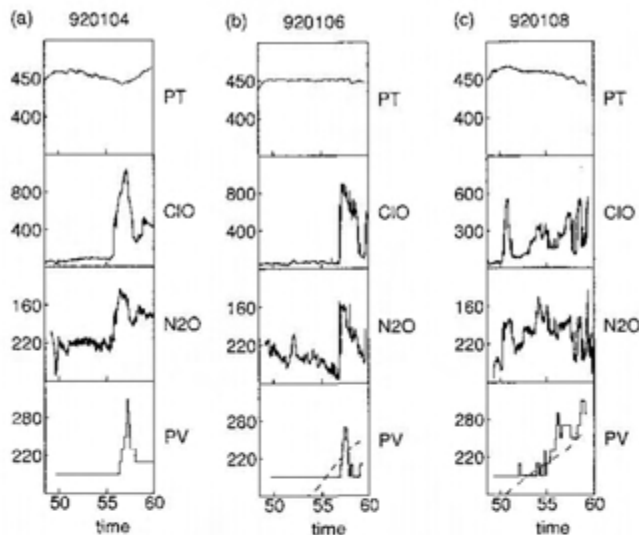


**Figure 2.** Data for northbound leg of ER-2 flights on (a) January 4, 1992; (b) January 6, 1992; and (c) January 8, 1992, as a function of universal time (kiloseconds). See Figure 1 for flight paths. Top to bottom: Potential temperature (K), ClO (parts per trillion by volume), and N<sub>2</sub>O (parts per billion by volume) as measured aboard the ER-2; and PV from the CAS calculation (solid curve) and NMC analyses (dashed curve). PV is in units of  $10^{-7} \text{ K m}^2 \text{ s}^{-1} \text{ kg}^{-1}$ . Note that there are no NMC analyses on January 4, 1992.

January 8, 1992, flight was different from that on the two earlier flights. By this date the vortex had rotated so that the flight path crossed first the tip of the filament crossed on the two previous flights and then a region where several filaments are emerging from the vortex. The structure in this latter region is more complicated than that across a single filament. The chemical tracers for the flight on January 8, 1992, show several narrow regions of perturbed vortex air during the northbound leg (see Figure 2c). Although the CAS results show a rich fine-scale structure, detailed agreement between the CAS calculation and the observations is not as good as for the previous two flights. The structure in the region where the flight path enters the vortex is complex, and the differences between the cross-section from the CAS calculation and the observations may be caused by many factors, such as the time difference between the ER-2 measurements and the CAS calculation, small-scale structures missing from the initial distribution, removal of filamentary structures by the surgery procedure, and variations in the potential temperature of the ER-2 measurements.

The contours from CAS shown in Figure 1 are valid at UT = 43,200 s (1200 UT), whereas the ER-2 measurements were taken between 50,000 and 60,000 s. During this time interval the rotation of the vortex (and filaments) can cause a significant displacement of some of the structures. For example, if the contours from CAS valid at UT = 56,160 s on January 8, 1992, are used instead of those valid at UT = 43,200 s then the filaments at the vortex edge (i.e., the spikes around the 56,000-s mark in Figure 2c) are crossed 600 s earlier along the flight path and there is better agreement with the observed N<sub>2</sub>O values, while the first filament is no longer crossed. On the other hand, if the contours valid at an earlier time are used, the first filament is crossed earlier on the flight and has a larger cross section.

The structure along the flight track is thus sensitive not only to the exact timing of the flight but also to the accuracy with which the CAS calculation can predict the time of passage of individual features across the flight track. This in turn implies that differences in the structure along the cross section could be due to small errors in the wind field over the 13-day calculation.

To investigate the sensitivity of the filamentary structures in CAS calculations to the duration of the calculation and the initial distribution, we performed several CAS calculations starting from the analyzed PV at different dates between December 23, 1991, and January 1, 1992. All calculations show the same vortex evolution and have very similar filamentary structures. Figure 3 shows the contours on January 8, 1992, from four different calculations. The overall structure of the vortex is very similar in all four calculations, although there are differences at small scales. There is generally more fine-scale structure in the longer calculations, although some structures are lost through the surgery procedure; for example, the filament in the 90°–180°W quadrant is shorter in the longer calculations, as the end of the filament has been removed by surgery. Another noticeable difference between the 7-day calculation (Figure 3d) and the other calculations is the smaller amount of air that has been drawn in around the vortex through the breaking event over eastern Canada. This difference can be traced back to differences in the contours on January 1, 1992. The above breaking event had already started by this date but is not detected in the analyses (compare the edge of the vortex at 45°E on January 1, 1992, in Figures 1a and 1b), and this causes the CAS calculation starting from the January 1, 1992, analyses to draw in less air around the vortex than the CAS calculations starting from earlier dates (which capture the breaking on January 1, 1992).

To quantify the differences between the calculations, we compared the profiles along the flight paths. For the January 4 and 6, 1992, flights, during which the flight path crossed a filament clear of the vortex, there is only a small variation of the structure from that shown in Figure 2. For example, the variation in the position of the filament between the different calculations is less than 20 km. There is, however, a larger variation for the January 8, 1992, flight path (see Figure 4). As expected, there is more small-scale structure in the longer calculations, but there are also variations in the positions and widths of the regions of vortex air. Figures 3 and 4 highlight the sensitivity of the structure along cross sections: it is hard to see differences, even at small scales, in the contour maps from the three longest calculations in Figure 3, but the differences along a cross section can be significant.

Filamentary breaking events also occurred during the period January 31 to February 10, 1989. Figure 5 shows the results of a 440 K CAS calculation from January 31, 1989. This calculation suggests that, as in the period shown in Figure 1, air was ejected from the vortex in the form of thick filaments that did not roll up into distinct, coherent vortices. It also suggests that there was strong stirring, more vigorous than during the previous period, inside the vortex. There is good agreement on the shape of the polar vortex between the NMC analyses and the CAS calculation, but again there is very little sign of the filamentary wave breaking in the analyses (see Figure 5b).

There were ER-2 flights from Stavanger, Norway (59°N, 6°E), into the vortex on four consecutive days at the end of this period; flight paths are shown in Figure 5. The CAS

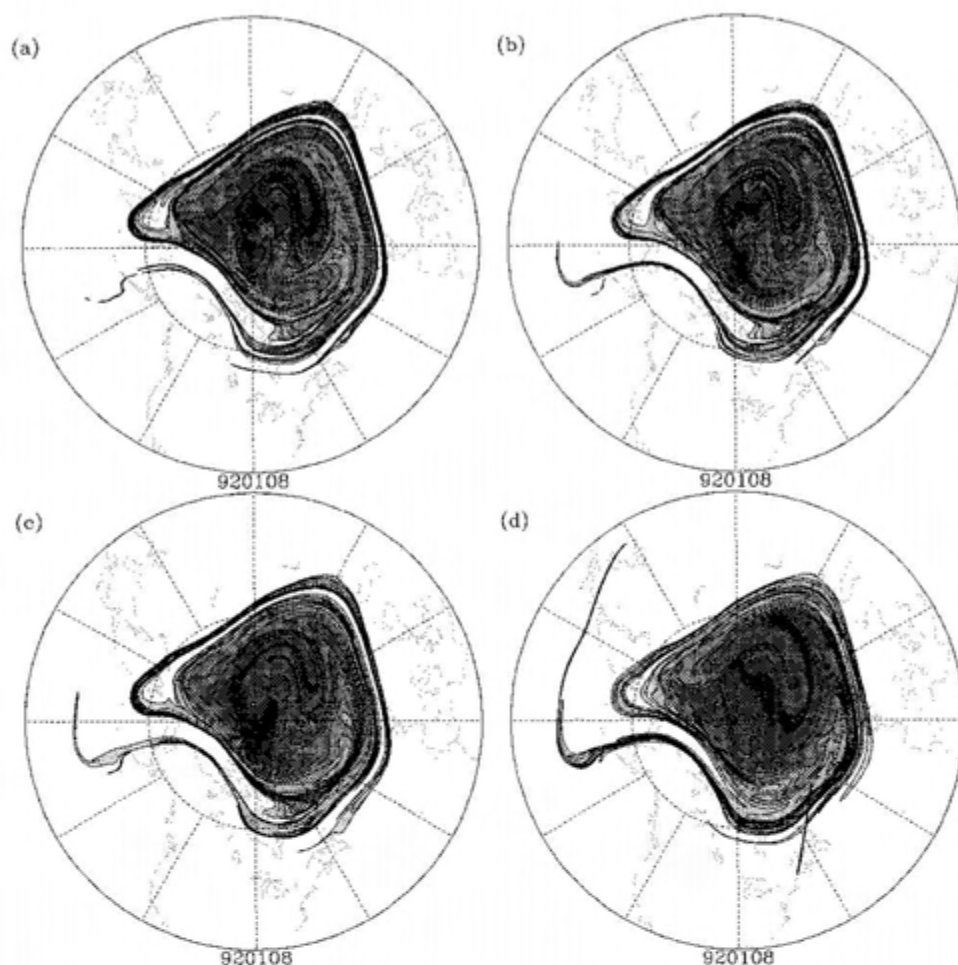


**Figure 3.** PV on the 450 K surface at 1200 UT on January 8, 1992, as determined from CAS calculations starting at (a) December 23, 1991; (b) December 26, 1991; (c) December 28, 1991; and (d) January 1, 1992. Contour levels are as in Figure 1.

calculation suggests that the first two flights crossed a filament of vortex air at the start of the flight path. The chemical tracers for these flights do indeed show perturbed vortex air outside the vortex. Figure 6a shows  $\text{ClO}$ ,  $\text{N}_2\text{O}$ , and wind speed measured on the northbound leg of the February 8, 1989, flight; the data from the return leg show similar structure. Also shown is the PV calculated from data measured aboard the ER-2 (see Hartmann *et al.* [1989] for details on the calculation of PV). Note that during this leg, the ER-2 is slowly descending and the potential temperature decreases from 470 to 450 K. Both the chemical tracers show spikes (scale < 100 km) at the start of the flight (UT  $\approx$  29,000 s) and near the vortex edge (UT  $\approx$  34,000 s). The PV calculated from ER-2 measurements starts after the first spike, but there is some indication of the second spike. Also shown in Figure 6 is the structure from the CAS calculation shown in Figure 5. Again, there is good qualitative agreement with ER-2 observations: the CAS results for February 8, 1989, show a filament at the beginning of the flight path, and for both of the February 8 and 10, 1989, flights there are fine-scale filaments at the vortex edge. There is a slight shift in the position of the structure from CAS and the ER-2 measurements. As stated earlier, this shift may be due to a variety of factors.

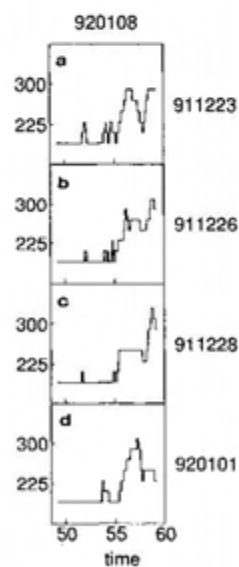


**Figure 4.** PV along flight path on January 8, 1992, as determined from CAS calculations starting at (a) December 23, 1991; (b) December 26, 1991; (c) December 28, 1991; and (d) January 1, 1992. Units are as in Figure 2.

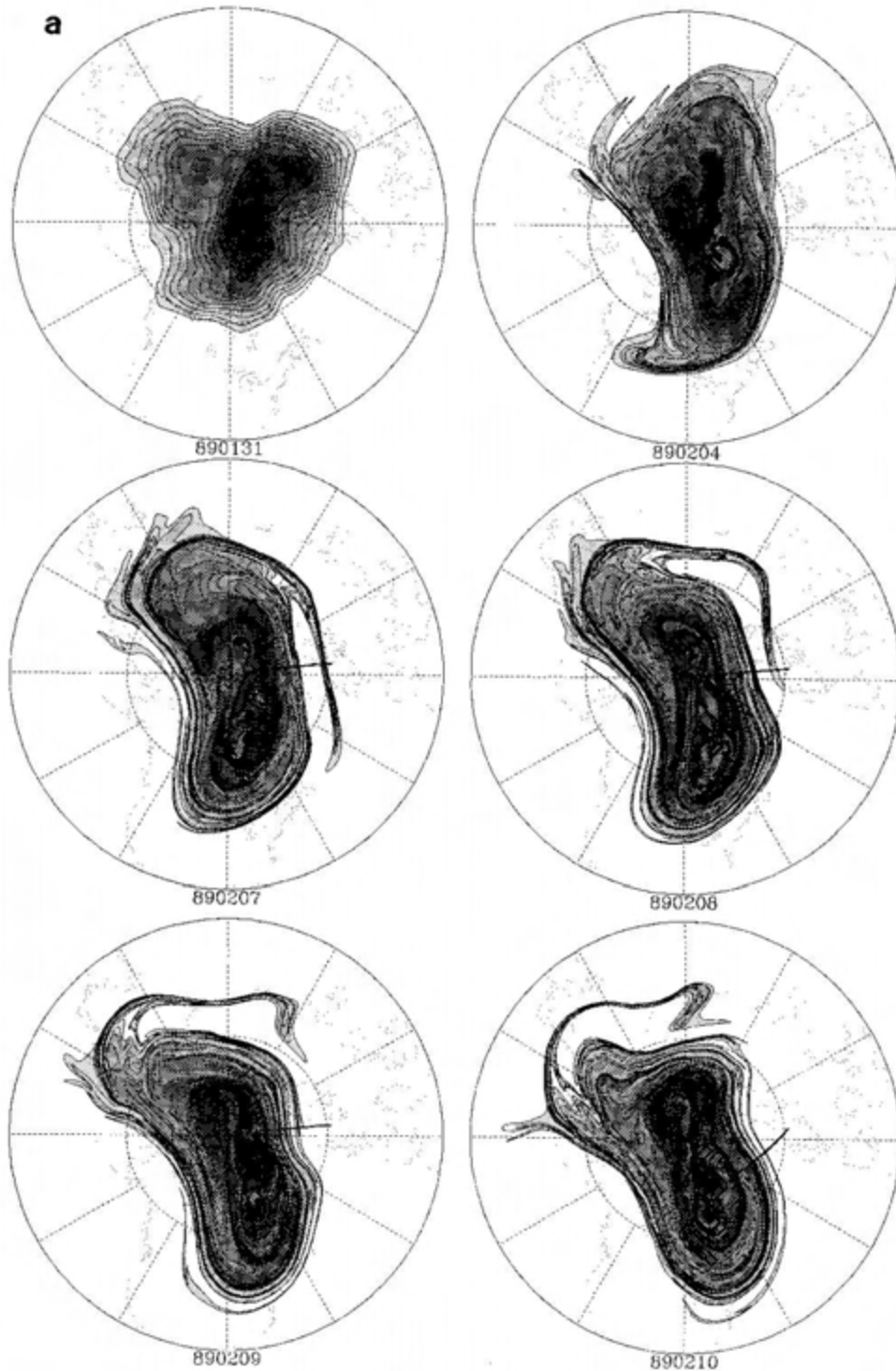


**Figure 5.** (a) Results of a CAS calculation from January 31, 1983, using NMC-analyzed winds on the 440 K isentropic surface. The initial contours are put at the analyzed locations of the  $(18, 20, 22, \dots) \times 10^{-6} \text{ K m}^2 \text{ s}^{-1} \text{ kg}^{-1}$  PV contours shown in Figure 5b. The ER-2 flight path is marked for each flight. (b) Ertel PV on the 440 K surface from NMC analyses on January 31 and February 10, 1989. Contour levels are as in Figure 5a.

The flight on February 8, 1989, has been examined by *Tuck et al.* [1992]. They compared the observed chemical tracers with ECMWF analyses and also came to the conclusion that the chemically perturbed air encountered by the ER-2 had been ejected from the vortex. Although there is a suggestion of the

ex-vortex air in the ECMWF analyses (Figure 2 of *Tuck et al.* [1992]), the filamentary structure of this feature is not shown. The difference between the high-PV blobs outside the vortex in ECMWF analyses and the features produced by CAS calculations is discussed further in section 7.

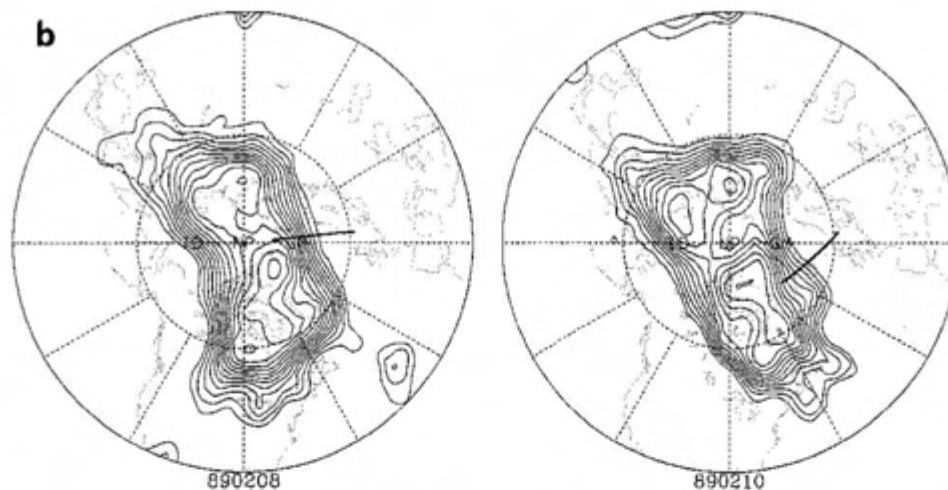


Figure 5. (continued)

Further CAS calculations suggest that during the period of the AASE missions there were many other wave-breaking events during which air was ejected from the vortex. In some of these events the breaking was more dramatic and larger amounts of vortex air were transported to midlatitudes (e.g., the breaking events at the end of January 1992 shown by *Plumb et al.* [this issue]). Unfortunately, the ER-2 did not fly through any of these regions, and we cannot confirm the reality of these events. However, aerosol data from DC-8 flights on January 22 and 23, 1992, do show the signature of vortex air outside the vortex. This period is examined in detail by *Plumb et al.* [this issue], and again the chemical measurements are consistent with CAS calculations and

confirm the reality of the filamentary wave breaking. Data from other DC-8 flights may confirm other breaking events, but we have yet to examine these data.

#### 4. Structure of the Vortex Edge

The CAS calculations for the periods of the AASE missions suggest that air was being ejected frequently from the lower stratospheric polar vortex in the form of long filamentary structures. The majority of the filaments were wrapped around the vortex, producing a narrow region outside the vortex where there were many filaments of ex-vortex air. The signature of this filamentary zone is observed in several ER-2 flights. These flights and the structure of the vortex edge are examined in this section.

We first consider the ER-2 ferry flights on February 20 and 21, 1989, when the ER-2 flew from Stavanger, Norway (59°N, 6°E), to Wallops Island, Virginia (38°N, 75°W), and then to Moffett Field, California (37°N, 122°W). On these two flights the ER-2 flew roughly parallel to the vortex edge and measured a large amount of fine-scale structure in the chemical tracers. These two flights have also been examined in detail by *Tuck et al.* [1992]. Figures 7a and 7b show the distribution on the 440 K isentropic surface on February 20, 1989, from a 10-day CAS calculation and NMC analyses. The vortex had split in two during the previous 2 days. During this split, a large number of filaments were generated, the majority being wrapped around the vortex. The filaments are not evident in the NMC analyses (Figure 7b), and there is only a hint of them in the ECMWF analyses (Figure 21 of *Tuck et al.* [1992]). Also note that during the split, air was entrained into the vortex. This entrainment is similar to that which occurred in February 1992 [*Plumb et al.*, this issue]. However, in 1989 the two parts did not merge to form a single polar vortex as they did in 1992; the 1989 event was the beginning of the vortex breakdown.

According to the CAS calculation, the flight path on February 20, 1989, crossed through these filaments, barely penetrated the vortex, and then exited into the surrounding filaments again (see Figure 7). The chemical tracers for this flight (Figure 8) are consistent with this picture: there are several spikes of perturbed vortex air at the beginning of the

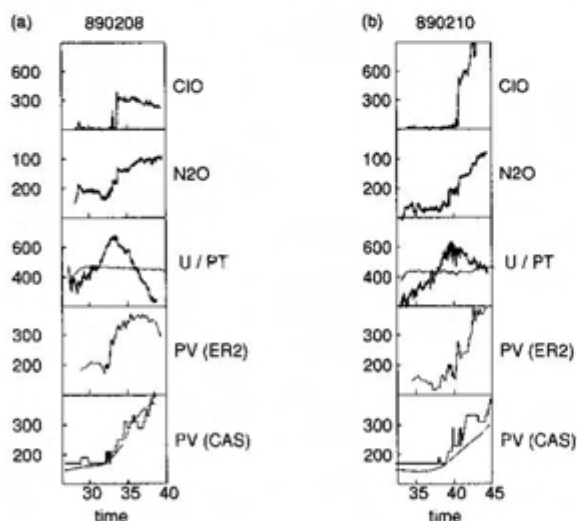
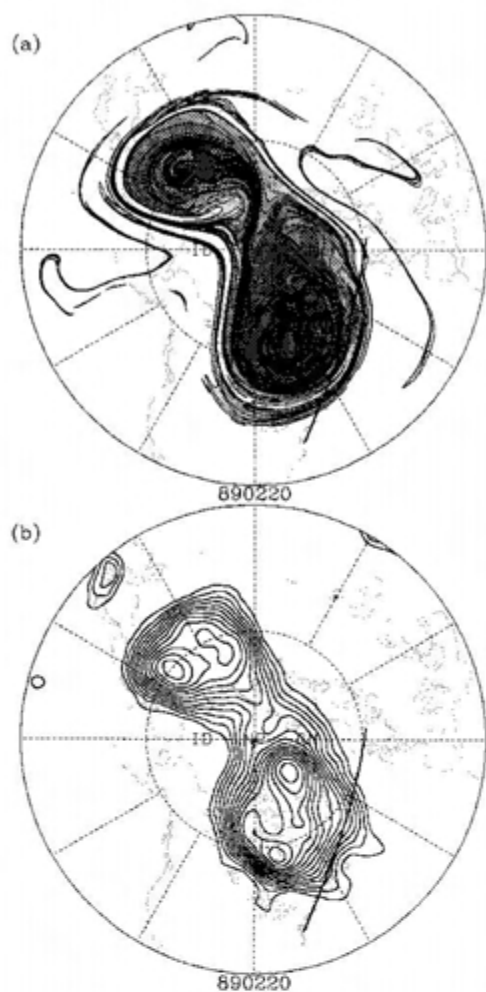


Figure 6. Data for northbound leg of ER-2 flight on (a) February 8, 1989, and (b) February 10, 1989, as a function of universal time (kiloseconds). See Figure 5 for flight path. Top to bottom: C1O (parts per trillion by volume), N<sub>2</sub>O (parts per billion by volume), wind speed (0.1 m/s) and potential temperature (kelvins) as measured aboard the ER-2, PV as calculated from measurements aboard the ER-2, PV from the CAS calculation (solid curve) and NMC analyses (dashed curve).



**Figure 7.** (a) Contours on February 20, 1989, from a 440 K CAS calculation starting 10 days earlier; (b) PV on the 440 K isentropic surface on February 20, 1989, from NMC analyses. Contour levels are as in Figure 5.

flight, a region of perturbed vortex air during the middle of the flight, and spikes of perturbed vortex air at the end of the flight. There is, however, more fine-scale structure in the ER-2 measurements than were captured by the CAS calculation, particularly at the beginning of the flight (Figure 8c). As mentioned in the previous section, there are many possible reasons for the differences between a cross section derived from CAS calculations and from aircraft observations.

To investigate the effect of the structure of the initial PV contours on the structure along the February 20, 1989, flight path, we repeated the calculation shown in Figure 7 using the result of the CAS calculation shown in Figure 5 as the initial conditions instead of the contours from the NMC analyses on February 10, 1989 (i.e., we continued the calculation shown in Figure 5 for 10 more days). This means that there are now fine scales in the PV distribution on February 10, 1989 (compare Figures 5a and 5b), and hence more fine-scale structure in the resulting CAS calculation. The structure along the flight path for this calculation is shown in Figure 8d. There is more fine-scale structure than in the previous CAS calculation but still less than in the observations.

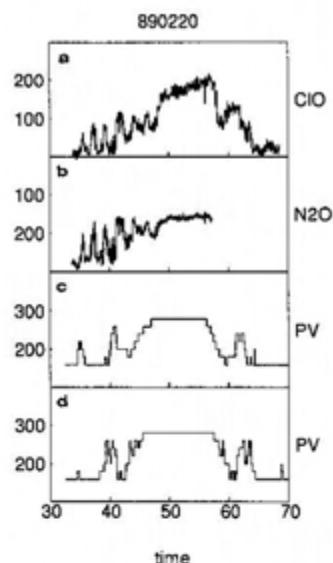


**Figure 8.** Data for ER-2 flight on February 20, 1989: (a) CIO (in parts per trillion by volume) and (b)  $N_2O$  (in parts per billion by volume) as measured aboard the ER-2, and PV from 440 K CAS calculation starting (c) 10 and (d) 20 days earlier. Potential temperature along flight is approximately 450 K.

On the February 21, 1989, flight from Wallops Island to Moffett Field, the flight path was outside the vortex, but according to the CAS calculation, it again crossed through surrounding filaments (see Figure 9). The filaments crossed contain air only from the very outer edge of the vortex. The chemical tracers on this flight again show fine-scale structure (Figure 10) and are consistent with the picture from CAS. Note that the peak  $N_2O$  values are characteristic of air at the very outer edge of the vortex. The agreement between the cross section from CAS and the chemical tracers is rather poor, possibly because of the choice of initial contours used in the CAS calculation. If extra, lower valued PV contours had been used in the calculation, there would have been more small-scale structure in the profile and maybe better agreement with the observations.

The above period is an extreme event in which the vortex is highly disturbed and many more filaments are produced than in "quieter" (more typical) periods. However, fine-scale filaments were generated in all CAS calculations performed. Several other ER-2 flights detected fine-scale structure, although less than in the above flights, at the vortex edge, for example, flights on January 19 and February 8 and 10, 1989, and January 20, 1992. CAS calculations during these periods show fine-scale filaments wrapping around the vortex, and these filaments are qualitatively consistent with the observations (e.g., Figure 6). (Note that there is no fine-scale structure at the vortex edge in the CIO for the February 10, 1989, flight, but both the  $N_2O$  and  $O_3$  (Figure 12 of Tuck *et al.* [1992]) do show fine-scale structure. This absence of high CIO could be because of CIO recovery through solar exposure [Schoeberl *et al.*, 1993; Webster *et al.*, 1993].)

Low-resolution meteorological analyses suggest the vortex edge as a region of large, monotonic PV gradient. By contrast, in situ tracer observations, these CAS calculations,

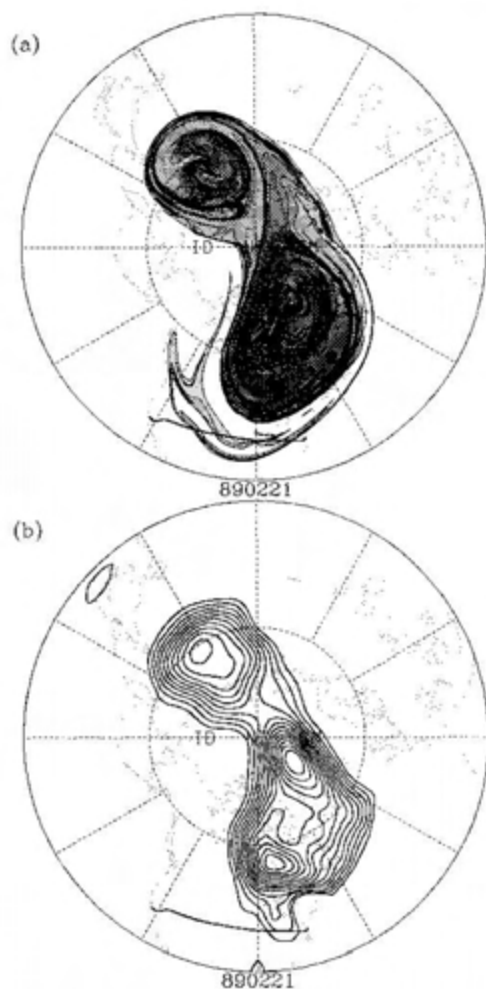


**Figure 9.** (a) Contours on February 21, 1989, from a 500 K CAS calculation starting 12 days earlier. The initial contours in the CAS calculations were the analyzed locations of the  $(35, 40, 45, \dots) \times 10^{-6} \text{ K m}^2 \text{ s}^{-1} \text{ kg}^{-1}$  PV contours. (b) PV on the 500 K isentropic surface on February 21, 1989, from NMC analyses. Contour levels are as in Figure 9a.

and high-resolution numerical simulations indicate that the edge region often has a rich fine-scale structure. Even though the gradients of PV and material tracers are very sharp, the edge region frequently contains multiple vortex filaments strung around the jet, and thus at these scales the gradients are not monotonic across the edge region. The concept of a single, sharp edge is a low-resolution concept, much like the large-scale view of a surface front as a temperature discontinuity. Therefore it is difficult to locate the edge at the high resolution of the CAS calculations.

Previously, the edge of the vortex has been defined using the maximum wind speed [e.g., Proffitt *et al.*, 1989; Kawa *et al.*, 1990] or a PV contour from analyses [e.g., Tuck *et al.*, 1992], but these smoothed quantities do not capture the fine-scale structure. For example, the wind speed calculated aboard the ER-2 [Chan *et al.*, 1990] on the February 8 and 10, 1989, flights is shown in Figure 6. From this we see that the maximum wind speed occurs at the outside edge of the filamentary structure and not at the edge of the region within which there are no reversed meridional gradients of PV. A similar displacement can occur if a smoothed PV distribution

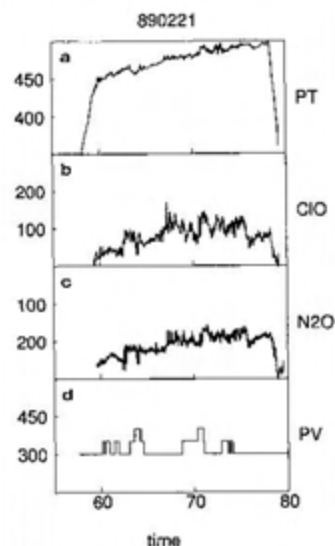


**Figure 10.** Data for ER-2 flight on February 21, 1989: (a) potential temperature (kelvins) of flight, (b) CIO (parts per trillion by volume) and (c)  $\text{N}_2\text{O}$  (parts per billion by volume) as measured aboard the ER-2; (d) PV from 500 K CAS calculation starting 13 days earlier.

is used to define the edge. Figure 11 shows a low-resolution picture (approximately  $4^\circ$  latitude  $\times$   $5^\circ$  longitude) for February 10, 1989, generated from a CAS calculation. There are no filamentary structures at this resolution, and the overall picture is similar to the NMC analyses (see Figure 5). If the vortex edge is defined using a contour from this smoothed distribution, then this edge is somewhere in the filamentary zone surrounding the vortex (depending on the contour value chosen). The difficulties in defining the edge of the vortex are discussed further in section 6.



**Figure 11.** Smoothed PV on February 10, 1989, from CAS calculation shown in Figure 5a. The PV is formed on a  $4^\circ$  latitude  $\times$   $5^\circ$  longitude using the contours from the CAS calculation. The PV =  $(18, 20, 22, \dots, 32) \times 10^{-6} \text{ K m}^2 \text{ s}^{-1} \text{ kg}^{-1}$  contours are shown.

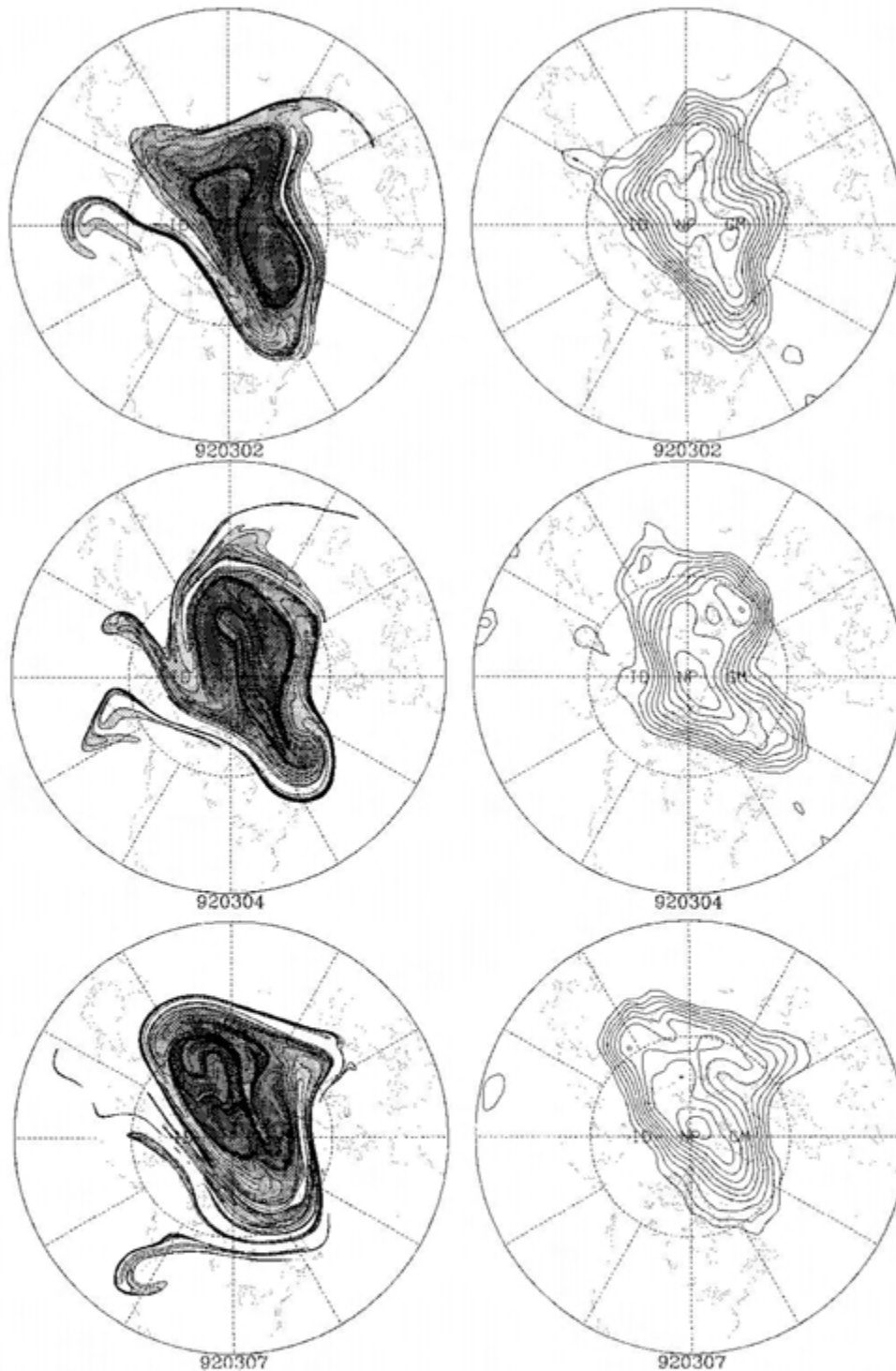


**Figure 12.** Ertel PV on the 450 K isentropic surface at 1200 UT on March 2, 4, and 7, 1992, from (left) CAS calculation from February 25, 1992, and (right) NMC analyses. PV contours equal (20, 22, 24, ...)  $\times 10^{-6} \text{ K m}^2 \text{ s}^{-1} \text{ kg}^{-1}$ .

### 5. Roll-Up of Filamentary Vorticity

The calculations shown in the previous sections suggest that the air ejected from the vortex during wave breaking seldom rolls up to form distinct, coherent vortices. There were, however, occasional events in which an ejected filament rolled up to form a small vortex. These events are discussed in this section.

Figure 12 shows a CAS calculation and the NMC analyses covering the period March 2–7, 1992. During this time there was a large breaking event in which air was ejected from the vortex at 150°E, 60°N on March 2, 1992. This air formed a thick filament, the end of which subsequently rolled up into a small vortex. This newly formed vortex survived for only 2 days, and by March 7, 1992, it had been stretched out into a thin filament.

This sequence of events cannot be easily observed in the NMC analyses. Although the small vortex does appear as a blob in the analyses on March 4, 1992, there is no sign in the analyses for the previous or next day (not shown), and there is very little evidence of any filamentary structures.

During the periods January 24–28 and February 22–28, 1992, similar breaking events occurred: a filament of air was ejected from the vortex, and the end of the filament formed a small vortex which survived for only a few days. These two events, which occurred soon after the entrainment of midlatitude air into the vortex, are examined by *Plumb et al.* [this issue].

The three periods discussed above were the only times during the AASE missions when filament roll-up was observed in CAS calculations. In all other cases of wave breaking, the air remained filamentary, with no sign of coherent vortices. This may be the result of the inability of CAS to properly simulate the roll-up of filaments [*Waugh and Plumb, 1993*]. However, the lack of roll-up near the polar vortex is consistent with numerical simulations [e.g., *Juckes and McIntyre, 1987; Waugh, 1993*] and with analysis of the stability of strips of PV in a straining flow [*Dritschel, 1989b; Waugh and Dritschel, 1991; Dritschel et al., 1991; Dritschel and Polvani, 1992*]. The stability analysis shows that the straining flow due to the polar vortex can suppress the instabilities that cause the roll-up into vortices. Roll-up occurs only when the filaments are in a region of very low strain. Furthermore, if filament roll-up does occur near the polar vortex (e.g., Figure 12), the newly formed vortex is unlikely to survive very long in the flow dominated by the polar vortex [*Dritschel and Waugh, 1992*].

## 6. Quantification of Stirring and Transport

In this section we quantify the stirring inside and outside the vortex and also the amount of air transported out of the vortex. The rate of stirring is here defined to be the rate of growth of the length of material contours. The more rapidly the contours lengthen, the stronger the stirring is. Similar contour length calculations have been performed in numerical simulations by *Norton [1993], Pierce and Fairlie [1993], and Bowman [1993]*. The amount of air transported out of the vortex during wave breaking is estimated by calculating the area of material contours that are outside the vortex but have PV characteristic of the vortex.

Fine-scale filamentary features are important in calculating the lengthening of contours and the area of contours outside the vortex; both quantities will be underestimated if these features are not resolved. Therefore we have repeated some of the previous CAS calculations without surgery and with twice the particle density.

Figure 13 shows the length of several material contours in CAS calculations covering the two periods examined in section 3: December 28, 1991, to January 11, 1992 (Figure 13a), and January 31 to February 12, 1989 (Figure 13b). Note the logarithmic vertical axis. These plots show that during both periods, there is rapid lengthening for contours outside or at the edge of the vortex (Figure 13a,  $PV \leq 24$ ; Figure 13b,  $PV \leq 28$ ), and hence there is very strong stirring in these regions. The contour length of exterior contours increases approximately exponentially, with an  $e$ -folding time of around 4–6 days. This is consistent with the studies by *Norton [1993]* and *Pierce and Fairlie [1993]*, both of

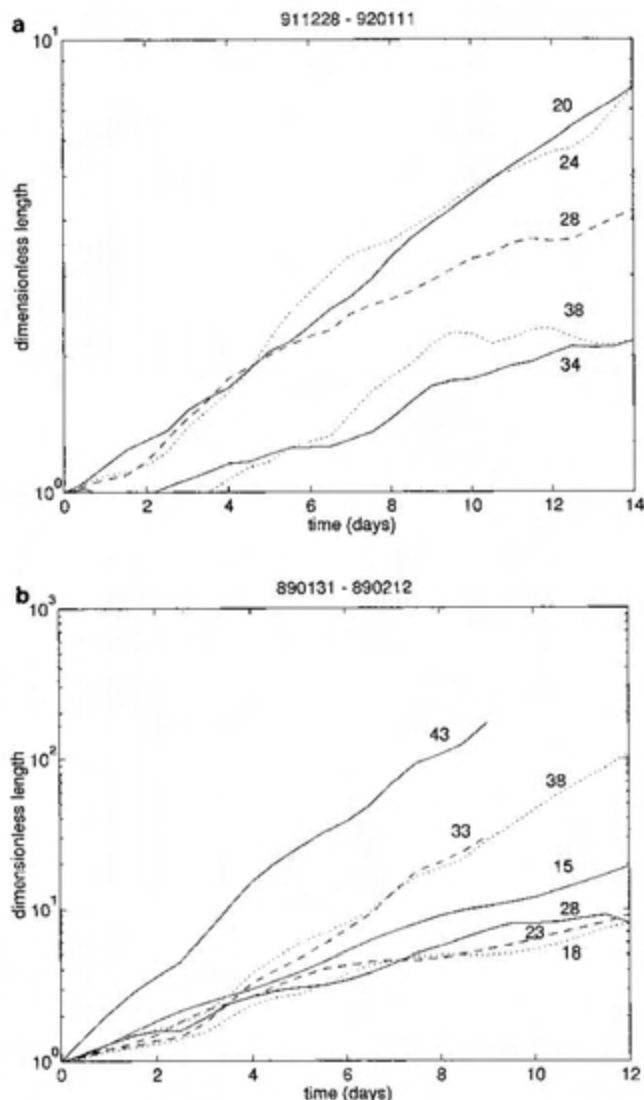


**Figure 13.** Length of material contours for (a) December 28, 1991, to January 11, 1992, and (b) January 31 to February 12, 1989. The value of the PV (in units of  $10^{-6} \text{ K m}^2 \text{ s}^{-1} \text{ kg}^{-1}$ ) of the contour is above each curve.

whom calculated  $e$ -folding times of around 4 days for contours outside the vortex in their numerical simulations.

*Norton [1993]* and *Pierce and Fairlie [1993]* found that the lengths of interior contours inside the vortex increased only slowly in their numerical studies, either linearly or exponentially, with  $e$ -folding times of at least 20 days, and hence there was only weak stirring. The calculations shown in Figure 13 suggest, however, that this may not always be the case in the real stratosphere. Whereas the interior contours lengthen only slowly during the period December 28, 1991, to January 11, 1992, with  $e$ -folding times between 12 and 16 days, the corresponding contours lengthen very rapidly during the period January 31 to February 12, 1989. In fact, during this time the interior contours lengthen more rapidly than those outside the vortex, and the length of the innermost contour has an  $e$ -folding time of less than 2 days. This implies very vigorous stirring inside the vortex, as can be seen in Figure 5.

Strong stirring inside the vortex is also observed in CAS

calculations of other periods during the AASE missions. For example, during the three entrainment events examined by *Plumb et al.* [this issue], there was a large amount of stirring inside the vortex. During the late January 1992 entrainment event (January 16–28, 1992), the contours inside the vortex lengthen exponentially, with  $e$ -folding times between 3 and 5 days. The periods during which there is strong internal stirring occur during large-amplitude wave events, and during these events the polar vortex is highly distorted. Note that there is also strong interior stirring in numerical simulations in which the vortex is highly distorted [e.g., *Juckes, 1987; Plumb et al., this issue*].

The exponential lengthening of material contours corresponds to a rapid decrease in the cross-flow horizontal scale of tracer features. In the presence of vertical shear, there will also be an accompanying decrease in vertical scales. It is this reduction in vertical scales that is likely to bring features down to molecular-diffusive scales and produce mixing between different constituents [*McIntyre, 1990*]. (Note that breaking inertio-gravity waves are also likely to be important in bringing about vertical mixing.) The rapid lengthening of contours outside and inside the vortex in the above calculations suggests that mixing of tracers may be occurring both outside and inside the Arctic vortex.

We now describe calculations to quantify the transport of air out of the vortex during breaking events. To quantify the transport out of or into the vortex, it is necessary to define the vortex boundary. But as discussed in section 4, the CAS calculations have shown that there are filaments surrounding the vortex and there is no continuous sharp edge. It is therefore difficult to define a boundary. If the vortex boundary is defined as the boundary within which there are no reversed meridional PV gradients, then all the filamentary structures will be outside the vortex (even if they are "trapped" in the polar jet and are being wrapped around the vortex core). On the other hand, if the boundary is defined to enclose the filaments of the high PV that are wrapped around the vortex core, then the so-called vortex includes filaments of high and low PV. Using a critical value of smoothed PV, or the maximum wind speed, results in a vortex boundary somewhere in between the above boundaries. The results of any quantification of transport out of and into the vortex will depend on what vortex boundary definition is used and also on the value of PV used in the boundary definition.

With this caveat, we define the vortex boundary by applying the "coarse-graining" procedure of *Waugh [1992]* [see *Dritschel and Waugh, 1992*] to the CAS contour initialized at the PV = 24 contour. In this procedure the surgical part of the contour surgery algorithm is applied repeatedly, with successive increases of the surgical cutoff scale, stopping at approximately 600 km. This procedure efficiently removes filamentary structures and isolates the vortex core. The PV = 24 contour was used in the boundary definition because this PV contour agrees well with the observed perturbed CIO (see next section).

We have thus estimated transport out of the vortex during a series of 9- to 12-day periods that cover the duration of AASE 2; Table 1 shows the area of air transported out of the vortex both as a percentage of the vortex area and as a percentage of the total area between the vortex and 30°N. During most of this period the wave breaking was weak and there was very little transport out of the vortex; typically, only a few percent of the vortex are transported out in a

**Table 1.** Area of Air Transported out of the Vortex Expressed as Percentage

Period	P <sub>1</sub>	P <sub>2</sub>
Dec. 6–18, 1991	1	0
Dec. 16–26, 1991	1	0
Dec. 23, 1991 to Jan. 2, 1992	5	1
Jan. 1–11, 1992	7	2
Jan. 7–17, 1992	3	1
Jan. 16–28, 1992	31	7
Feb. 2–11, 1992	2	0
Feb. 9–19, 1992	0	0
Feb. 19–28, 1992	15	3

P<sub>1</sub>, area as a percentage of the vortex area; P<sub>2</sub>, area as a percentage of the area between the vortex and 30°N.

10-day period. There were, however, two periods when there were strong wave breaking and large transport out of the vortex: January 16–28, 1992 (Figure 3 of *Plumb et al.* [this issue]), and February 19–28, 1992 (Figure 12 of *Plumb et al.* [this issue]). These two events accounted for the majority of the transport out of the vortex from December 1991 to February 1992. Note that the amount of air transported out of the vortex in these events was still only a small proportion of the total mass in middle latitudes; for example, the air transported from the vortex during all breaking events in January 1992 accounts for only about 9% of the area between the vortex and 30°N.

We also calculated the transport out of the vortex during the two periods in AASE 1 examined in this paper. The amounts of air transported out of the vortex during the January 31 to February 10 and February 10–21, 1989, periods were 4 and 7%, respectively, of the vortex area. This corresponds to only 1 and 2%, respectively, of the area between the vortex and 30°N and is smaller than the transport determined by *Tuck et al. [1992]* from ECMWF PV analyses.

## 7. Discussion

The CAS calculations in this paper suggest that Rossby wave breaking is a frequent occurrence in the northern hemisphere wintertime lower stratosphere. This wave breaking transfers air out of the polar vortex in the form of long filamentary structures. The reality of these filamentary structures and the accuracy of the CAS calculations have been confirmed by comparisons with observations of chemical tracers aboard the ER-2; see also comparisons by *Plumb et al.* [this issue] with aerosol observations made aboard the DC-8. The ejected air in the CAS calculations seldom rolls up into vortices, suggesting that filaments are ubiquitous in the lower Arctic stratosphere. The majority of these filaments are wrapped around the vortex rather than being mixed into a broad "surf zone" as in the middle stratosphere (see below). This causes the vortex to be partly or even totally surrounded by a narrow region of fine-scale filaments, and there is seldom a sharp edge around the whole vortex. This makes it difficult to define the vortex edge. The air removed is primarily stripped from the outer edge of the vortex, and only a small amount of air is removed from deep inside the vortex. However, the CAS calculations together with contour length calculations have also shown that strong

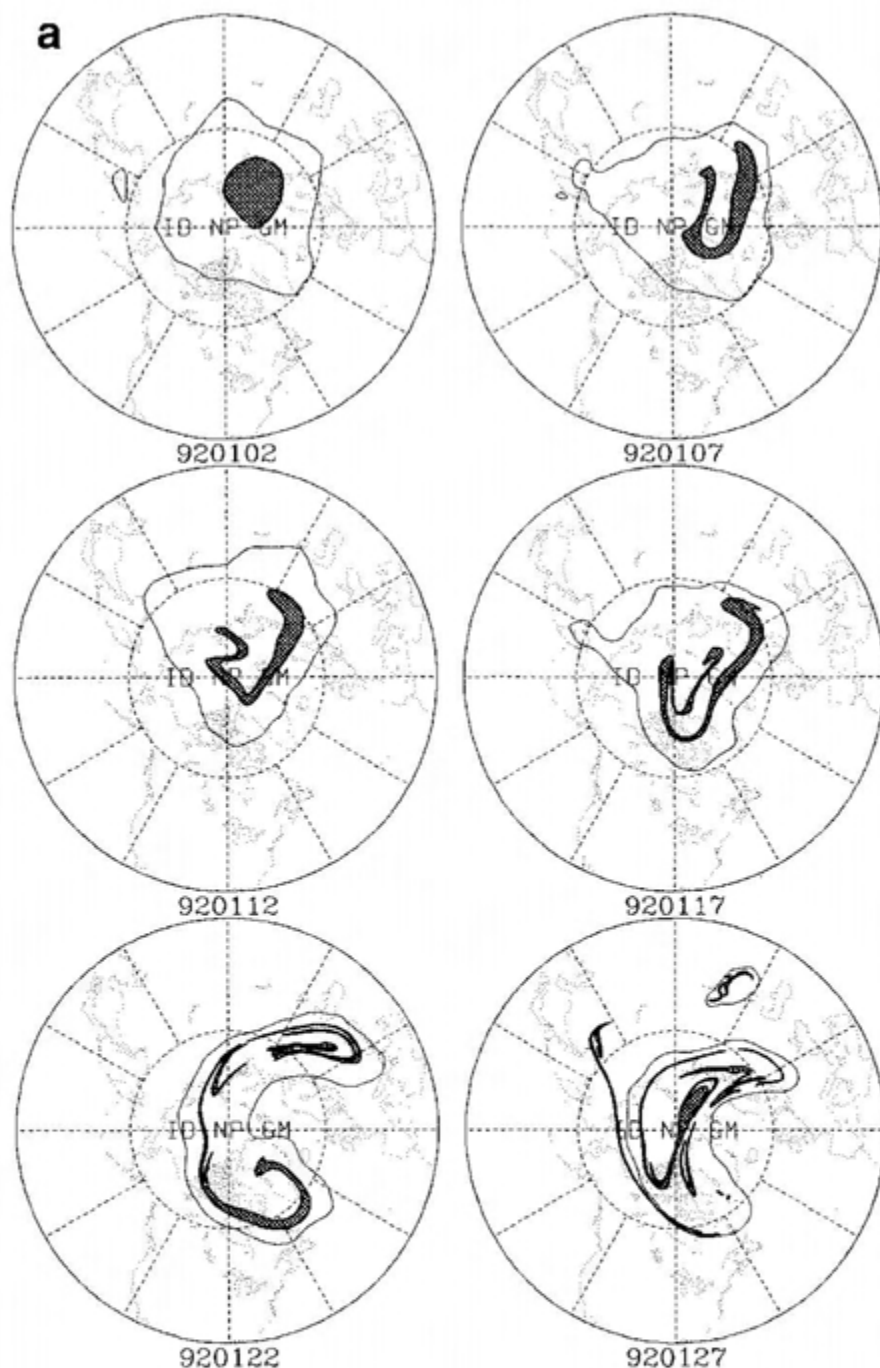


**Figure 14.** Evolution of 195 K temperature contour from a 450 K CAS calculation initialized on (a) January 2, 1992, and (b) January 21, 1992. The initial contours are put at the NMC-analyzed locations of the 195 K contour. Shaded regions correspond to the CAS calculation, while light contours correspond to the analyzed  $PV = 2.5 \times 10^{-5} \text{ K m}^2 \text{ s}^{-1} \text{ kg}^{-1}$  contour.

stirring can occur inside the vortex. This interior stirring means that air at the outer edge of the vortex may have previously been at the center of the vortex.

An example of this stirring and subsequent breaking is shown in Figure 14a. This shows the results of CAS calculation where the initial contour coincides with the analyzed 195 K temperature contour on the 450 K isentropic surface on January 2, 1992. The region with a temperature lower than 195 K is the approximate region where polar stratospheric clouds are expected to form and hence is the

possible origin of chemically perturbed air [Newman *et al.*, 1993]. The material evolution of this region gives an indication of the evolution of the chemically perturbed air that was perturbed on January 2, 1992. Figure 14a shows that the perturbed air is initially inside the vortex (the shaded regions correspond to the CAS calculation, while the light contours correspond to the analyzed  $PV = 25$  contours), but through internal stirring the perturbed air reaches the vortex edge by the latter part of this period. (Note that the internal stirring during the initial period is weaker than in many other periods

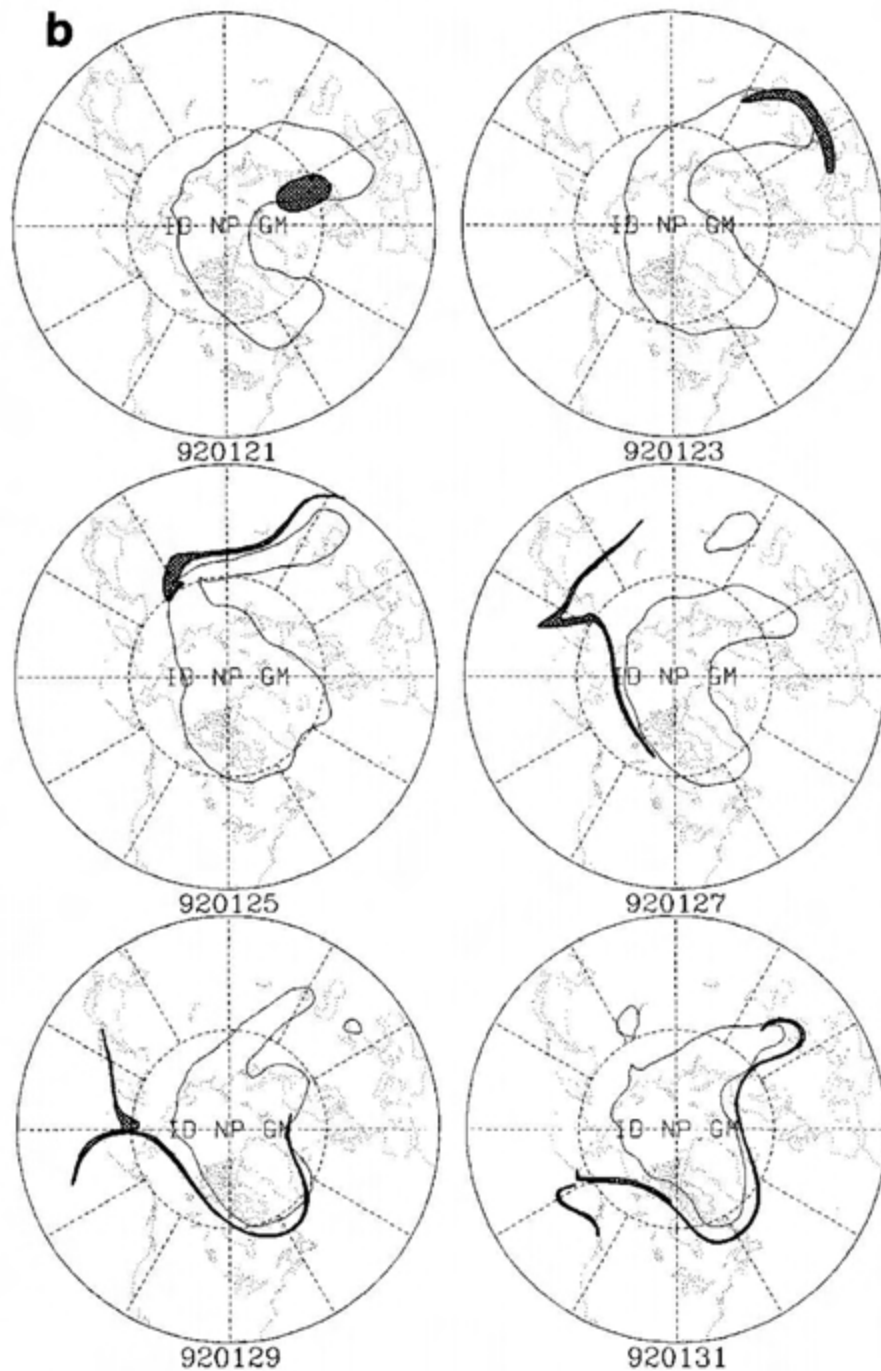
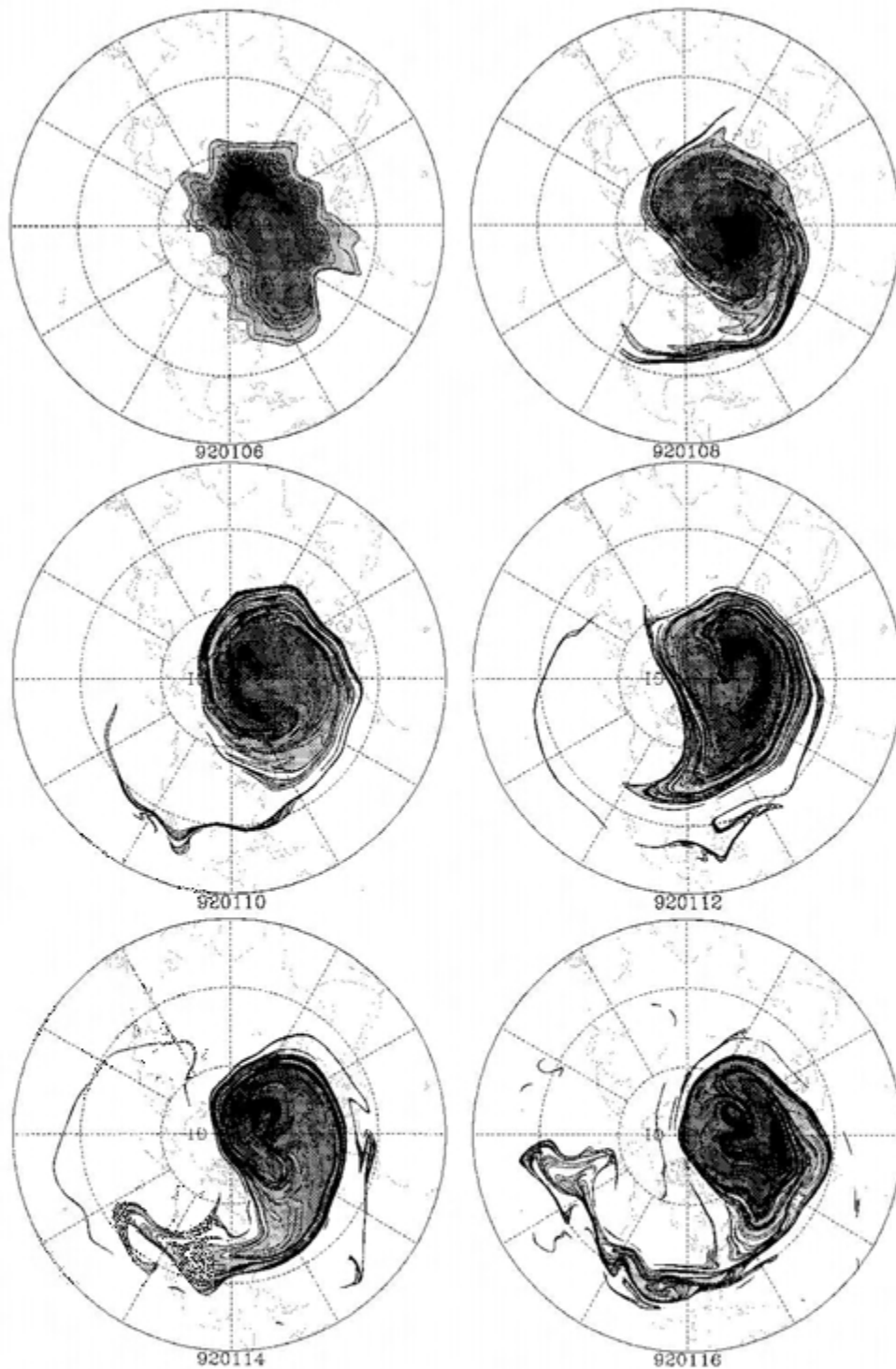


Figure 14. (continued)

during the AASE missions; see section 6.) Some of this perturbed air is then ejected from the vortex in the breaking events occurring at the end of the period [see *Plumb et al.*, this issue]. Figure 14b shows a similar CAS calculation for evolution of the air that was perturbed on January 22, 1992. The region of temperatures lower than 195 K is at the edge of the vortex on this date. (The temperature on the 450 K isentropic surface warms to above 195 K after this date.) The perturbed air is quickly stretched into a filament and swept around the vortex and into midlatitudes.

A series of CAS calculations similar to those shown in Figure 14 has been performed: one calculation was done for each day during the 1991–1992 winter during which there is

a region on the 450 K isentropic surface with temperature below 195 K (December 22, 1991, to January 21, 1992). The composite of the contours at a given date from all calculations in this series indicates the extent of the perturbed air at that date. This series of calculations shows that even though the temperature is below 195 K in only localized regions, the perturbed air has filled nearly all of the vortex by January 6, 1992. Furthermore, the evolution of perturbed air agrees well with the perturbed ClO observed by the microwave limb sounder instruments on the upper atmosphere research satellite [*Waters et al.*, 1993]. The evolution is also very similar to that for CAS calculations initialized with the PV = 24 contour, and the amount of perturbed air transported to



**Figure 15.** Results of a CAS calculation from January 6, 1992, using NMC-analyzed winds on the 850 K isentropic surface. The initial contours are put at the analyzed locations of the  $(35, 40, 45, \dots) \times 10^{-4} \text{ K m}^2 \text{ s}^{-1} \text{ kg}^{-1}$  PV contours on that surface.

midlatitudes during January 1992 is therefore similar to that calculated in section 6, that is, by January 31, 1992, around 9% of the area between the vortex and  $30^\circ\text{N}$  is perturbed air.

We have identified substantial transport of air out of the vortex in the form of filamentary structures during the AASE missions. The total amount of vortex air transported to midlatitudes during the period of AASE 2 was approximately

50% of the vortex area (see Table 1). During this period the area of the vortex remained approximately constant, suggesting that the vortex is being replenished through diabatic processes. (Note that the amount of midlatitude air transported into the vortex through intrusion events is only a few percent of the vortex area [Plumb *et al.*, this issue].) Although the presence of the above amount of perturbed

vortex air in midlatitudes might have a modest impact on midlatitude chemistry, this rate of isentropic midwinter transport is not sufficient to account for the 30-day turnover time claimed by Tuck *et al.* [1993]. Of course, we do not here take any account of vertical (diabatic) transport.

The calculations presented suggest that transport out of the vortex cannot be investigated by using low-resolution analyses alone, as these analyses do not resolve filamentary structures. The ECMWF analyses do, however, show a large number of small-scale features in midlatitudes with PV characteristic of the vortex, and these features have been associated with ejected vortex air [Tuck *et al.*, 1992]. However, the calculations in this paper cast doubt on the reality of many of these PV blobs. It has been shown that air ejected from the vortex is filamentary and seldom forms vortices (i.e., blobs). More importantly, the CAS calculations give no support for the position of the majority of high-PV blobs in the ECMWF analyses. For example, the ECMWF analyses for February 8, 20, and 21, 1989 (Figures 2, 21, and 18 in the paper by Tuck *et al.* [1992]) show a large number of blobs in midlatitudes (primarily in a subtropical jet stream, 20°–30°N), but the CAS calculations for these periods (see Figures 5, 9, and 11 in this paper) show very little evidence for these structures, particularly at low latitudes.

Finally, we discuss the differences between the wave breaking in the CAS calculations for the lower stratosphere and previous observational studies of wave breaking in the middle stratosphere [e.g., McIntyre and Palmer, 1983, 1984; Clough *et al.*, 1985; Leovy *et al.*, 1985]. These previous studies suggest that large tongues of air are ejected from the vortex during wave breaking and that this vortex air is transported to low latitudes, whereas the CAS calculations shown here suggest that the ejected air forms thin filaments which are usually wrapped around the vortex. The reason for this difference appears to be the different characteristics of the flow in the middle and lower stratosphere. As shown in Figure 15, CAS calculations on the 850 K isentropic surface show a picture similar to that in the above studies, that is, a comma-shaped vortex with a large tongue of air extending to low latitudes (the outer latitude in Figure 15 is 20°N). Note that there is a suggestion that this tongue may have rolled up into vortices. The 450 K calculation for the same period shows thin filamentary breaking as in Figure 1. The differences in the flow are possibly related to differences in the vortex structure (e.g., the presence of the subtropical jet in the lower stratosphere rather than a broad band of tropical easterlies), the increase in amplitude of upward propagating Rossby waves [Charney and Drazin, 1961; Dritschel and Saravanan, 1993], and the effect of subplanetary-scale tropospheric disturbances on the lower stratosphere. The vertical structure of the wave breaking in the stratosphere is currently under investigation.

**Acknowledgments.** Work at MIT has been supported by NSF through grant 9218841 and by NASA through grant NAGW-1727. Some computations were performed on the Cray Y-MP at the Pittsburgh Supercomputing Center through grant ATM920001P. The CAS code was developed from a contour surgery code kindly provided by David Dritschel. The authors thank Warwick Norton and Michael McIntyre for helpful discussions, an anonymous reviewer for helpful comments, and the entire AASE 2 team for support during the course of the experiment.

## References

- Bowman, K. P., Barotropic simulation of large-scale mixing in the Antarctic polar vortex, *J. Atmos. Sci.*, **50**, 2901–2914, 1993.
- Carver, G. D., W. A. Norton, and J. A. Pyle, A case study in forecasting the stratospheric vortex during EASOE, *Geophys. Res. Lett.*, in press, 1993.
- Chan, K. R., K. R. Bowen, T. P. Bui, S. G. Scott, and J. Jean-Day, Temperature and wind measurements and model atmospheres of the 1989 Airborne Arctic Stratospheric Expedition, *Geophys. Res. Lett.*, **17**, 1319–1339, 1990.
- Charney, J. G., and P. G. Drazin, Propagation of planetary-scale disturbances from the lower into the upper atmosphere, *J. Geophys. Res.*, **66**, 83–109, 1961.
- Clough, S. A., N. S. Grahame, and A. O'Neill, Potential vorticity in the stratosphere derived using data from satellites, *Q. J. R. Meteorol. Soc.*, **111**, 335–358, 1985.
- Dritschel, D. G., Strain-induced vortex stripping, in *Mathematical Aspects of Vortex Dynamics*, edited by R. E. Caflisch, p. 107, Society for Industrial and Applied Mathematics, Philadelphia, Pa., 1988.
- Dritschel, D. G., Contour dynamics and contour surgery: Numerical algorithms for extended, high-resolution modeling of vortex dynamics in two-dimensional, inviscid, incompressible flows, *Comput. Phys. Rep.*, **10**, 77–146, 1989a.
- Dritschel, D. G., On the stabilization of a two-dimensional vortex strip by adverse shear, *J. Fluid Mech.*, **206**, 193–221, 1989b.
- Dritschel, D. G., and L. M. Polvani, The roll-up of vorticity strips on the surface of a sphere, *J. Fluid Mech.*, **234**, 47–69, 1992.
- Dritschel, D. G., and R. Saravanan, Three-dimensional quasi-geostrophic contour dynamics, with an application to stratospheric dynamics, *Q. J. R. Meteorol. Soc.*, in press, 1993.
- Dritschel, D. G., and D. W. Waugh, Quantification of inelastic interactions of vortices in two-dimensional vortex dynamics, *Phys. Fluids A*, **4**, 1737–1744, 1992.
- Dritschel, D. G., P. H. Haynes, M. N. Jukes, and T. G. Shepherd, The stability of a two-dimensional vortex filament under uniform strain, *J. Fluid Mech.*, **230**, 647–666, 1991.
- Hartmann, D. L., K. R. Chan, B. L. Gary, M. R. Schoeberl, P. A. Newman, R. L. Martin, M. Loewenstein, J. R. Podolske, and S. E. Strahan, Potential vorticity and mixing in the south polar vortex during spring, *J. Geophys. Res.*, **94**, 11,625–11,640, 1989.
- Jukes, M. N., Studies of stratospheric dynamics, Ph.D. thesis, Cambridge Univ., Cambridge, England, 1987.
- Jukes, M. N., and M. E. McIntyre, A high-resolution one-layer model of breaking planetary waves in the stratosphere, *Nature*, **328**, 590–596, 1987.
- Kawa, S. R., D. W. Fahey, L. C. Anderson, M. Loewenstein, and K. R. Chan, Measurements of total reactive nitrogen during the Airborne Arctic Stratospheric Expedition, *Geophys. Res. Lett.*, **17**, 485–488, 1990.
- Legras, B., and D. G. Dritschel, Vortex stripping and the generation of high vorticity gradients in two-dimensional flows, *Appl. Sci. Res.*, **51**, 445–455, 1993.
- Leovy, C. B., C.-R. Sun, M. H. Hitchman, E. E. Remsburg, J. M. Russell, L. L. Gordley, J. C. Gille, and L. V. Lyjak, Transport of ozone in the middle stratosphere: Evidence for planetary wave breaking, *J. Atmos. Sci.*, **42**, 230–244, 1985.
- Loewenstein, M., J. R. Podolske, K. R. Chan, and S. E. Strahan, Nitrous oxide as a dynamical tracer in the 1987 Airborne Antarctic Ozone Experiment, *J. Geophys. Res.*, **94**, 11,589–11,598, 1989.
- Loewenstein, M., J. R. Podolske, K. R. Chan, and S. E. Strahan, N<sub>2</sub>O as a dynamical tracer in the arctic vortex, *Geophys. Res. Lett.*, **17**, 477–480, 1990.
- McIntyre, M. E., Middle atmospheric dynamics and transport: Some current challenges to our understanding, in *Dynamics, Transport and Photochemistry in the Middle Atmosphere of the Southern Hemisphere*, edited by A. O'Neill, pp. 1–18, Kluwer Academic, Norwell, Mass., 1990.
- McIntyre, M. E., and T. N. Palmer, Breaking planetary waves in the stratosphere, *Nature*, **305**, 593–600, 1983.
- McIntyre, M. E., and T. N. Palmer, The 'surf zone' in the stratosphere, *J. Atmos. Terr. Phys.*, **46**, 825–849, 1984.
- McIntyre, M. E., and T. N. Palmer, A note on the general concept of wave breaking for Rossby and gravity waves, *Pure Appl. Geophys.*, **123**, 964–975, 1985.
- Newman, P. A., L. R. Lait, M. R. Schoeberl, E. R. Nash, K. Kelly,

- D. Fahey, R. M. Nagatani, D. Toohey, L. Avallone, and J. Anderson, Stratospheric meteorological conditions in the Arctic polar vortex, 1991 to 1992, *Science*, **261**, 1143-1146, 1993.
- Norton, W. A., Breaking Rossby waves in a model stratosphere diagnosed by a vortex-following coordinate system and a contour advection technique, *J. Atmos. Sci.*, in press, 1993.
- Pierce, B. R., and T. D. A. Fairlie, Chaotic advection in the stratosphere: implications for the dispersal of chemically perturbed air from the polar vortex, *J. Geophys. Res.*, **98**, 18,589-18,595, 1993.
- Plumb, R. A., D. W. Waugh, R. J. Atkinson, P. A. Newman, L. R. Lait, M. R. Schoeberl, E. V. Browell, A. J. Simmons, and M. Loewenstein, Intrusions into the lower stratospheric Arctic vortex during the winter of 1991-1992, *J. Geophys. Res.*, this issue.
- Polvani, L. M., and R. A. Plumb, Rossby wave breaking, filamentation and secondary vortex formation: The dynamics of a perturbed vortex, *J. Atmos. Sci.*, **49**, 462-476, 1992.
- Proffitt, M. R., et al., A chemical definition of the boundary of the Antarctic ozone hole, *J. Geophys. Res.*, **94**, 11,437-11,448, 1989.
- Salby, M. L., R. R. Garcia, D. O'Sullivan, and P. Callaghan, The interaction of horizontal eddy transport and thermal drive in the stratosphere, *J. Atmos. Sci.*, **47**, 1647-1665, 1990.
- Schoeberl, M. R., et al., The evolution of ClO and NO along air parcel trajectories, *Geophys. Res. Lett.*, **20**, 2511-2515, 1993.
- Stolarski, R. S., P. Bloomfield, R. D. McPeters, and J. R. Herman, Total ozone trends deduced from Nimbus 7 TOMS data, *Geophys. Res. Lett.*, **18**, 1015-1018, 1991.
- Stolarski, R. S., R. Bojkov, L. Bishop, C. Zerefos, J. Staehelin, and J. Zawodny, Measured trends in stratospheric ozone, *Science*, **256**, 342-349, 1992.
- Toohey, D. W., W. H. Brune, K. R. Chan, and J. G. Anderson, In situ measurements of midlatitude ClO in winter, *Geophys. Res. Lett.*, **18**, 21-24, 1991.
- Toohey, D. W., L. M. Avallone, L. R. Lait, P. A. Newman, M. R. Schoeberl, D. W. Fahey, E. L. Woodbridge, and J. G. Anderson, The Seasonal Evolution of Reactive Chlorine in the Northern Hemisphere Stratosphere, *Science*, **261**, 1134-1136, 1993.
- Tuck, A. F., et al., Polar stratospheric cloud processed air and potential vorticity in the northern hemisphere lower stratosphere at mid-latitudes during winter, *J. Geophys. Res.*, **97**, 7883-7904, 1992.
- Tuck, A. F., J. M. Russell, and J. E. Harries, Stratospheric dryness: Antiphased desiccation over Micronesia and Antarctica, *Geophys. Res. Lett.*, **20**, 1227-1230, 1993.
- Waters, J. W., et al., Stratospheric chlorine monoxide and ozone from the MLS on the UARS, *Nature*, **362**, 597-602, 1993.
- Waugh, D. W., The efficiency of symmetric vortex merger, *Phys. Fluids A*, **4**, 1745, 1992.
- Waugh, D. W., Contour surgery simulations of a forced polar vortex, *J. Atmos. Sci.*, **50**, 714-730, 1993.
- Waugh, D. W., and D. G. Dritschel, The stability of filamentary vorticity in two-dimensional geophysical vortex-dynamics models, *J. Fluid Mech.*, **231**, 575-598, 1991.
- Waugh, D. W., and R. A. Plumb, Contour advection with surgery: A technique for investigating fine scale structure in tracer transport, *J. Atmos. Sci.*, in press, 1993.
- Webster, C. R., et al., Hydrochloric loss and chlorine chemistry on polar stratospheric clouds in the Arctic winter, *Science*, **261**, 1130-1134, 1993.
- R. J. Atkinson, R. A. Plumb, and D. W. Waugh, Center for Meteorology and Physical Oceanography, Massachusetts Institute of Technology, 54-1726, Cambridge, MA 02139.
- L. M. Avallone, Department of Chemistry, Harvard University, Cambridge, MA 02138.
- L. R. Lait, P. A. Newman, and M. R. Schoeberl, NASA Goddard Space Flight Center, Greenbelt, MD 20771.
- M. Loewenstein, NASA Ames Research Center, Moffett Field, CA 94035.
- R. D. May and C. R. Webster, Jet Propulsion Laboratory, Pasadena, CA 91109.
- D. W. Toohey, Department of Geosciences, University of California, Irvine, CA 92717.

(Received April 19, 1993; revised August 26, 1993; accepted September 9, 1993.)